

EXPERIMENTAL AND COMPUTATIONAL RESEARCH ON THE FIRE BEHAVIOR OF RESTRAINED REINFORCED CONCRETE COLUMNS – PART II

Ataman HAKSEVER*

Emeritus (2006) from Trakya University, Çorlu Faculty of Engineering, Tekirdağ, Turkey

Abstract: In the eighties, the work was particularly focused in SFB (Sonder Forschungs Bereich: A special fire research activity for structural elements in Braunschweig Technical University, 1971-1986) on the development of a universal material model for normal concretes for fire case. Through a comprehensive mathematical description of the rheological phenomena at elevated temperatures, the relaxation behavior of restrained columns could be successfully predicted. It aimed at clarifying the difference, which took place between the lateral deformation behavior as well as restraint forces of calculated and measured reinforced concrete columns (RFC) under fire conditions. Such a material model was developed, in fact, through close cooperation of sub-projects A and B3 of SFB.

Naturally, the use of such material model requires an immense computational treatment. Theoretical studies have shown, however, that this is worthwhile, because only by this process the fire behavior of structural concrete elements can be taken into account satisfactorily. It should be stressed here that a material model can gain confidence only if it has been tested successfully under different boundary conditions. In particular, the model must apply for the assessment of the fire behavior of structural elements in large scale.

In this regard, relaxation tests on reinforced concrete columns under different boundary conditions have been carried out in the special furnace of SFB. The heating of the reinforced concrete columns have been made with respect to ISO834 Fire as well as to a simulated fire condition. The following paragraphs describe the tests and also their theoretical investigation.

Keywords: Structural fire safety, reinforced concrete columns, fire resistance, relaxation, fire behavior

RECHERCHE EXPÉRIMENTALE ET COMPUTATIONNELLE SUR LE COMPORTEMENT DES COLONNES EN BÉTON ARMÉ RESTREINTES SOUMIS AU FEU – PART II

Résumé: Dans les années quatre-vingt le travail en SFB (Sonder Forschungs Bereich: Une activité spéciale de recherche sur le feu pour les éléments structurels de l'Université Technique de Braunschweig, 1971 à 1986) a été particulièrement axée sur le développement d'un modèle de matériau universel pour le béton normaux en cas d'incendie. Il visait à la clarification de la différence, qui a eu lieu dans la mesure et le comportement de la latérale déformation calculée de colonnes en béton restreint sous l'action du feu. Grâce à une description mathématique globale des phénomènes rhéologiques à des températures élevées, l'estimation de la réponse de relaxation de colonnes restreints pu être estimée avec succès. Un tel modèle matériau a été développé, en fait, par une coopération étroite des sous-projets A et B 3 de SFB.

Naturellement, l'utilisation d'un tel modèle de matériau nécessite un énorme traitement de calcul. Les études théoriques ont montré, cependant, que cela vaut un tel coût. Parce que par ce procédé comportement au feu d'éléments structuraux en béton être estimé satisfaisante. Il convient de souligner ici que d'un modèle de matériau peut gagner la confiance que si elle a été testé avec succès sous différentes conditions aux limites. En particulier, le modèle doit appliquer pour l'évaluation du comportement au feu des éléments structuraux en formats pratiques.

À cet égard essais de relaxation sur des colonnes en béton armé sous différentes conditions aux limites ont été réalisées dans le four spécial de SFB. Le chauffage des colonnes en béton armé ont été apportées par rapport à la norme ISO834-le Feu ainsi que d'une condition de feu simulé. Les paragraphes suivants décrivent les essais ainsi que leur traitement numérique.

Mots clés: Structural sécurité en cas d'incendie, colonnes en béton armé, résistance et comportement au feu, relaxation

1. Introduction

In SFB, 1971-1986 (see references) of the Technical University of Braunschweig fundamental research were carried out in the eighties, to clarify the discrepancy, which occurred in the measured and the calculated lateral deformation behavior of restrained (RFC) under fire exposure (see Figure. 4.1). The work was particularly focused on the development of a universal material model for normal concrete. Through a comprehensive mathematical description of the rheological phenomena at elevated temperatures, the relaxation behavior of restrained columns could be successfully predicted. Such a material model was developed, in fact, through close cooperation of subprojects A and B3 of SFB (Haksever, A., 1984-1986, *Mathematische Modellierung*, part I and Schneider, U., 1982, Klingsch, W, 1975., Diss).

Naturally, the use of such material model requires a complicated and enormous computational treatment. The computational studies have shown, however, that such a research is worthwhile, because only by this process fire behavior of restrained structural concrete elements can be predicted satisfactorily. It should be stressed here that a material model can gain confidence only if it has been tested successfully under different boundary conditions (see Anderberg, Y., 1976) In particular, the model must apply for the assessment of the fire behavior of structural elements in large scale (see dimensions of specimens in paragraph 4). In the literature, various material models for concretes can be found. In many cases, however, the verification of such models lacks for the case of fire, especially when a restraint is present for large scale structural elements caused by the entire structure interaction.

In this regard, relaxation tests on (RFC) under different boundary conditions have been carried out in the special furnace of SFB. The heating of the reinforced concrete columns have been made with

respect to ISO834 Fire as well as to a simulated fire exposure. The following paragraphs describe the tests and also their theoretical treatment.

1.1. Literature review

Concerning literature, it is rare to find fire test results on the structural columns under restraining conditions especially for (RFC). These tests are conducted mainly for steel columns and a restraint is simulated longitudinally as well as rotationally.

Truong-Thang Nguyen, Kang Hai Tan, 2014, analyze thermal-induced restraint forces in (RFC) subjected to eccentric loads. Analytical and numerical analyses are conducted in this paper to investigate the additional axial forces induced in eccentrically-loaded (RFC) that are restrained from thermal elongation in concrete framed structures when a fire occurs. A simplified analytical model to directly determine these so-called thermal-induced restraint forces is proposed based on the concepts of equivalent distributed temperature as well as eccentricity and temperature-dependent reduction factor of axial stiffness.

Kang-Hai Tan, Truong-Thang Nguyen, 2013, investigate structural behaviors of (RFC) subjected to uniaxial bending and restraint at elevated temperatures. A total of six specimens were tested to failure to investigate the effects of uniaxial bending, axial restraint, and initial load level on the structural behaviors of (RFC) at elevated temperatures. Temperature-dependent axial deformations, lateral deformations, thermal-induced restraint forces, failure modes, and failure times of the test specimens are compared with those obtained from numerical analyses using SAFIR program. It is experimentally shown that the lateral deformation at elevated temperatures is adversely affected by uniaxial eccentricity and initial load level. A simplified analytical model to directly determine these so-called thermal-induced restraint forces is proposed based on the concepts of equivalent distributed temperature as well as eccen-

tricity and temperature-dependent reduction factor of axial stiffness.

P. Bamonte, F. Lo Monte, 2015, present in their paper the performance of EN 1.4003 ferritin stainless steel hollow columns (ENV 1992 1-2) when exposed to fire loading. Tubular thin-walled members were considered in this study because structural applications of ferritin stainless steels generally incorporate such profiles. Fire loading was applied under a constant concentrically compressive load. Identical column tests at room temperature are also reported.

António José P. Moura Correia, João Paulo C. Rodrigues, 2012, investigate the behavior of steel columns subjected to fire depending on their interaction with the surrounding building structure. To improve knowledge of the phenomenon a great many fire resistance tests have been carried out on steel columns with restrained thermal elongation. The results showed that increasing the stiffness of the surrounding structure may not lead to a reduction of the column's critical temperature. This is because, associated with an increase of the axial stiffness is an increase of the rotational stiffness, which has an opposite effect to the first one.

I. Cabrita Neves, J.C. Valente, J.P. Correia Rodrigues, 2002, make a proposal, based on the results of a series of tests and calculations, with the aim of being used as a simple method to correct the value of the critical temperature of steel columns free to elongate, in order to take into account the restraint effect of the structure to which they belong in a practical situation. A simple model is presented and used in a qualitative analysis.

David Lange, Johan Sjöström, 2014, describe in their paper the effect of thermal exposure varying in both the horizontal and vertical axes to columns by means of including this thermal boundary in a solution of classical Euler beam theory. The resulting solution allows for a variation in the stiffness of the rotational restraint at both ends of the column and a non-uniform

temperature exposure through the column's section and along its height.

1.2. Comments about the given references

Some cited references might be too old in this paper (especially from SFB). Although some researchers are doing some similar works just now, it is intended to demonstrate that the SFB had been aware even in eighties about the problematic of restraint columns and developing restraint forces during the fire as well as prediction of these forces and deformations. However, test and computational research results have not been published up to now because a constitutional material model was missing and it was a forth going main research activity of the author.

It must be pointed out here that research in SFB is mainly focused on the verification of the material laws in case of restraint of (RFC) and aimed at especially a systematical investigation as large scale specimens in 1:1 practical dimensions. SFB furnace was constructed mainly for this purpose. In this concern by holding the (RFC) in vertical condition it is held a uniformly heating of the test specimen and conformity with the practical conditions in the furnace (see Figure 3.2).

2. Calculation Method

A three dimensional explicit-discretization method is used for the computational treatment of (RFC) for fire case. That means the temperature distribution is calculated in each time step from the previous time step of the temperature distribution. Time steps are chosen for ISO834 Fire as 10 sec. as well as for constant heating. A two-dimensional discretization is applied in order to calculate the temperature distribution in the cross section of the concrete and reinforcing steel temperatures are determined bound to their location with respect to the cross section temperatures. Heat transfer conditions are taken into account in case of nonsteady state temperature development in the furnace (see appendix C).

A one-dimensional discretization is used along the height of (RFC). In each discrete element, the curvatures are calculated bound to the acting bending moment and axial load with respect to the second order theory, using the material model at elevated temperatures. Lateral deformations at each discrete element are calculated by means of the *force method*. Stability analyses are carried out with small time steps (appr. 3 min.) in order to achieve a good convergence. In the simulation the failure criterion are taken into account as stability failure or material failure (fracture). Every failure is ended naturally with a fracture situation.

A stability failure is present in the simulation when the calculated lateral deformations increase also in case of slightly reducing the attained axial restraint forces in the simulation. This situation is indicated that the lateral deformations boundless increase in iterations under acting forces and no any stability can be attained for (RFC) which cause at the end to a fracture in the most stressed cross section (see Figure e.g. 4.10...).

In case of material failure, development of the lateral-deformations doesn't show a boundless increase but a spontaneous fracture determines the fire resistance. Material failure is present when no any equilibrium for the critical cross section could be determined after 10 iterations. In this case the *load bearing capacity* of the cross section is calculated and compared with the acting external loading (see figure 4.4).

Both failure modes are also observed during the tests.

3. Planning of the Parameters of the Tests

In the fire tests, three test parameters are mainly varied (Haksever, A., SFB, 1978-1980, Relaxationserhalten von Stahlbetontragwerke, 1981-1983, zum Relaxationsverhalten von Stahlbetonstützen). These parameters are similar to those that have been studied on the small specimens of the subproject B3 of SFB (Schneider, U., 1979, Creep

and relaxation and 1982, Behavior of concrete.) It is mainly temperature, controlled axial elongation and restraining of the specimens in case of fire. All the tests are carried out in Euler Case-II.

The heating of the (RFC) are made under different fire developments and restraint conditions. In controlling the axial elongation of the (RFC) during the fire, it is simulated both by a total as well as by a controlled restraining. By controlling test parameters temperature and elongation, restraint forces and lateral deformations are measured during the fire. In order to assess the reliability of the material model used, different test specimens are tested concerning cross sections and slenderness ratio. Application of the material model requires a successive calculation process by small time steps. In calculation steps, it was necessary to have information for the stress distribution in the cross section and lateral deformations of the column from the previous time step.

In the following paragraph, characteristic test and computational results are compared, so that both the effectiveness of the computer program, SARCOS (Structural Analysis of Reinforced Concrete Structures), as well as the reliability of the new material model used is clearly demonstrated.

3.1. Temperatures and vertical deformations of the test furnace

For the evaluation of computational models and for checking the results through tests the exact realization of the predetermined boundary conditions in the furnace is a precondition. The size of the deviations from the controlled values as temperature and loading is a measure of the quality and performance of a test furnace. In the special furnace of SFB it is succeeded to keep these deviations like temperature and restraining in all conditions as small as possible.

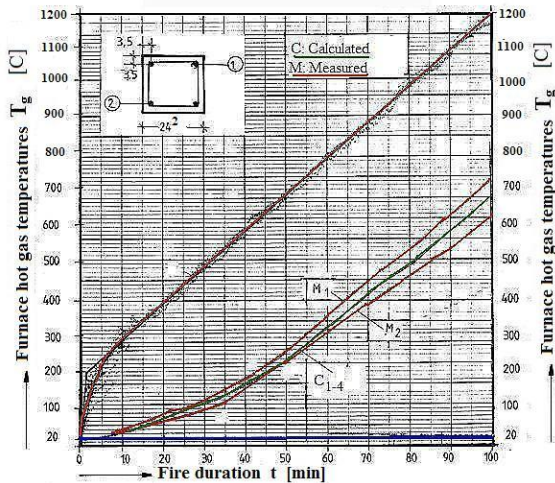


Figure 3.1: Furnace and calculated and measured (RFC) temperatures

In the relaxation tests carried out on (RFC) the fire exposure is applied, both in accordance with the standard temperature time curve - (according to ISO834 or DIN 4102, 1981) - and predetermined hot-gas temperature curve (here a constant heating rate). The Figure 3.1 illustrates that the hot-gas temperatures and the temperatures controlled are simulated satisfactorily. Also, at a heating rate \dot{T}_f of 10C(Δ K)/min for a ceiling height of 4.80 m of fire room, after short initial temperature disturbance, negligible lower deviations are measured along the column height. During the controlling of the temperature time curve according to ISO834 Fire the deviations run up from the predetermined curve max $\pm 30^\circ\text{C}$.

In Figure 3.1, the measured corner reinforcing steel temperatures of the tested (RFC) are also illustrated. The steel temperatures are recorded during the test simultaneously together with the hot-gas temperatures. Obviously between calculation and measurement a good agreement exists. It can be assumed, therefore, that the mathematical treatment of the temperature problem has been solved reliably with computer program SARCOS. In the test framework of the SFB the fire tests can be run load as well as axial elongation controlled. In case of axial *elongation-controlled* tests, the vertical deformations of the loading framework are also determined by appropriate

measurements. In Figure 3.2, the vertical deformation of the loading framework is shown depending on the axial load of the compression member (RFC). They are taken into account as additional axial elongation in the calculation beside the predetermined elongation. The predetermined elongation m_f of the reinforced concrete column is thus increased by the vertical deformation of the loading framework. The predetermined free restraint of the column is applied immediately after the initial loading of the concrete column with the beginning of the fire exposure. In the following paragraph, the calculation results with the test results are compared and discussed.

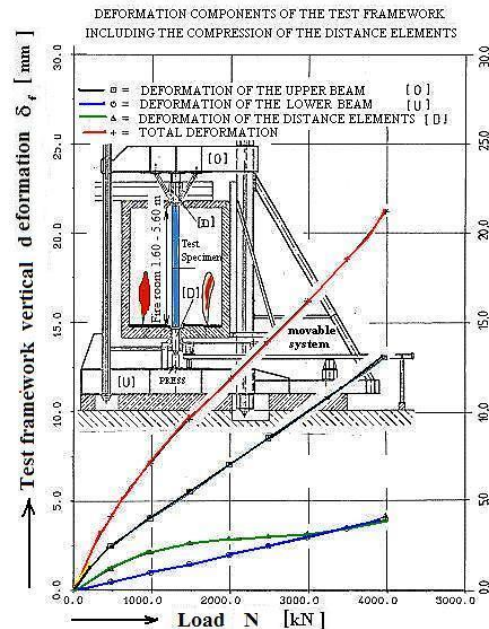


Figure 3.2: Vertical deformations of the framework due to loading of (RFC)

4. Discussion of the Calculation Results

In this paragraph, the results of restrained column tests are compared with the computational analysis respectively. Especially typical relaxation tests are chosen of which statically as well as thermally boundary conditions cover the most usual range from practice. Relaxation tests in SFB for the large-scale *framework columns* with 1:1 dimensions are however excluded from investigation in this paper.

4.1. Column test ST-1/1

The computational analysis of this test is discussed in detail in (Haksever, A., SFB, 1981-1983). In the mentioned report, the computational results are obtained through application two different material models and compared with the test results. The calculation results from the material model used up to now (Klingsch, 1975) showed a strong deviation among the test results in both the measured restraint forces as well as the measured lateral deformations in case of a *total restraining*. Figure 4.1 demonstrates this discrepancy.

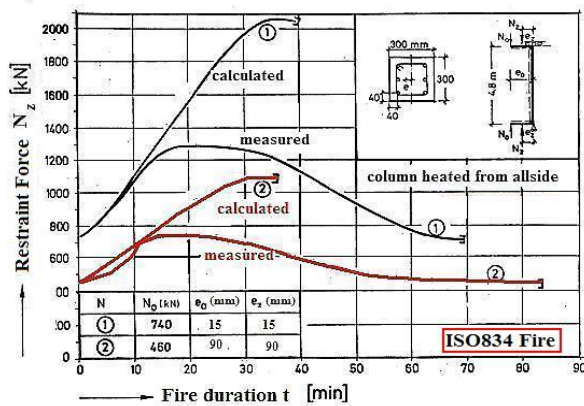


Figure: 4.1 Calculated and measured test results for different static conditions

In order to reduce the discrepancies between the calculated and measured restraint forces, instead of a total restraining, a certain controlled *free* elongation is planned during the fire. Although this process reduced the unagreement in the prediction of restraint forces between test and calculation, still the measured lateral deformations and the fire resistance of the column could not be satisfactorily reproduced by the calculation.

In Figure 4.2 the simulated elongation of the (RFC) is shown during the fire. The shaded area of the figure shows the additional deformation component of the loading frame work, which arises due to restraint axial force. Although this relaxation test is intended to carry out by simulating a total restraining, a negligibly small elongation is allowed in the calculation due to

convergence reasons. From Figure 4.2 it can be seen that this elongation attains after 90 minutes of fire exposure an allowable elongation of 0.1 %.

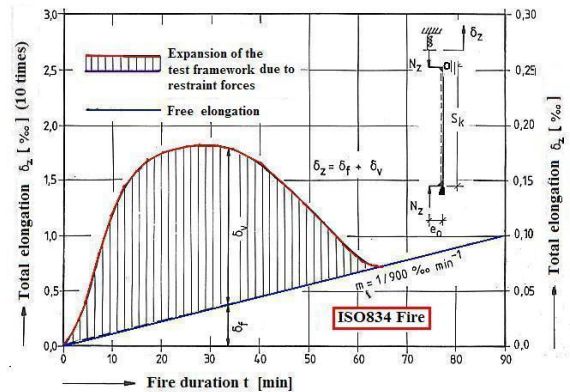


Figure 4.2: Total elongation of the framework due to free elongation and the restraining

The vertical deformation of the test facility is determined by the measured restraint forces using Figure 3.2. Figure 4.3 shows now the calculated forces using with the *new material model* together with the restraint forces measured in the fire test. Obviously a significant improvement is achieved in the prediction of the restraint forces by means of the application of the *material law* presented in PART I.

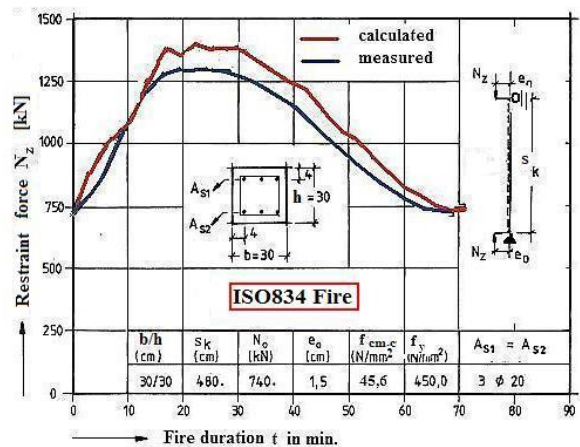


Figure 4.3: Calculated and measured restraint forces

However, the effectiveness and the validity of the material model used can only be verified, if also between the calculated and measured lateral deformations of the concrete column a good agreement exists. In Figure 4.4, the calculation results for lateral

deformations together with the measured test results are illustrated with respect to the fire duration. The deformation measurements are carried out at a certain height of (FRC) in the buckling direction. It is indeed that this good agreement between the calculation and the measurement exists also in failure mode. It can also be seen from Figure 4.4 that the fire resistance of the concrete column is also determined exactly by the calculation.

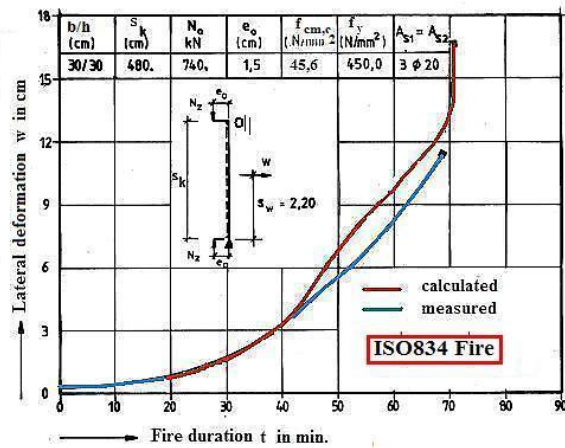


Figure 4.4: Measured and calculated lateral deformations

4.2. Column test ST-1/2.

In this test, a total restraining for the reinforced concrete column is simulated. The heating of the column is carried out on all sides according to ISO834. For the calculation of this test a small free elongation is taken into account as shown in Figure 4.5. The properties of the material used in room temperatures as well as the static boundary conditions of the reinforced concrete column are shown in Figure 4.6.

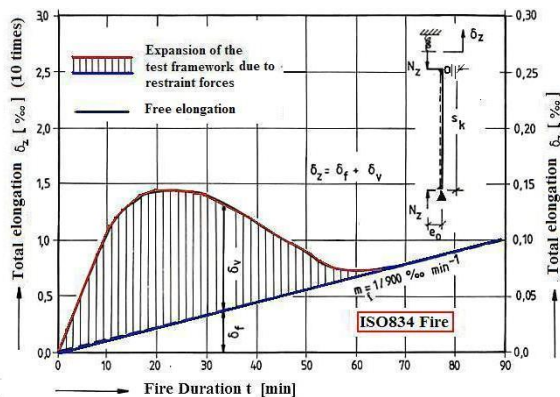


Figure 4.5: Total elongation of the framework due to free elongation and the restraining

The hatched area in Figure 4.5 represents the technically not prevented further axial deformations of the test framework (see Figure 3.2). Due to the relatively greater load eccentricity in comparison to the pretest, less restraint forces are developed during the fire exposure (comp. Figures 4.3 and 4.6).

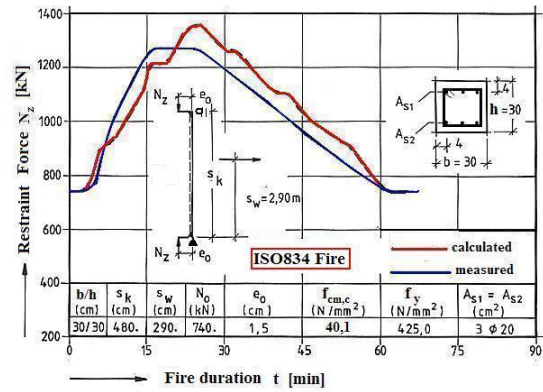


Figure 4.6: Measured and calculated restraint forces

Taking into account the boundary conditions shown in Figure 4.6, a computational analysis is carried out in order to compare the restraint forces and the lateral deformations measured in the test. Figure 4.6 shows the measured and calculated restraint forces over the fire duration. It can be seen that, even by a rather large load eccentricity (h/e = 20), the measured restraint forces are predicted satisfactorily in the calculation. However, the computational fire resistance time is tolerable less than as it is observed in the test.

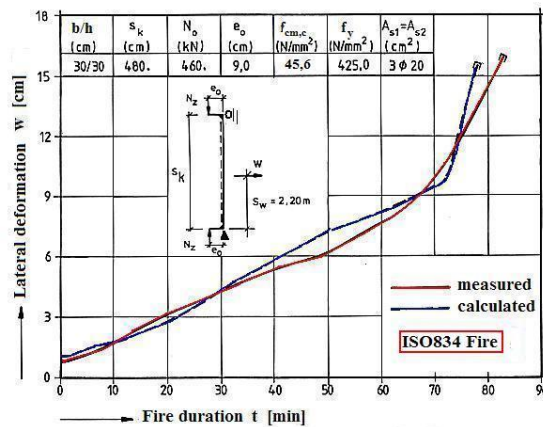


Figure 4.7: Measured and calculated lateral deformations

In the test the calculated and measured lateral deformations of the (RFC) over the fire duration are illustrated in Figure 4.7. It is well known that the development of the axial forces, in the case of restraining of (RFC), is decisively determined by the development of the lateral deformations. Therefore, a good agreement between the measured and calculated lateral deformations of the reinforced concrete column must exist for the fire case. It becomes clear that such a good agreement indeed exists between measurement and calculation; a proof that the developed material model in *PART I* reproduces the fire behavior of the (RFC) as realistically as possible and the effects from the second order theory are exactly included in the calculation program.

4.3. Column test B2-6

In this test also a free restraining for the (RFC) is applied during the fire. As it can be seen in Figure 4.8, planned restraining is controlled in such a way that a longitudinal elongation should attain the limit of 1 % after 90-minute fire duration.

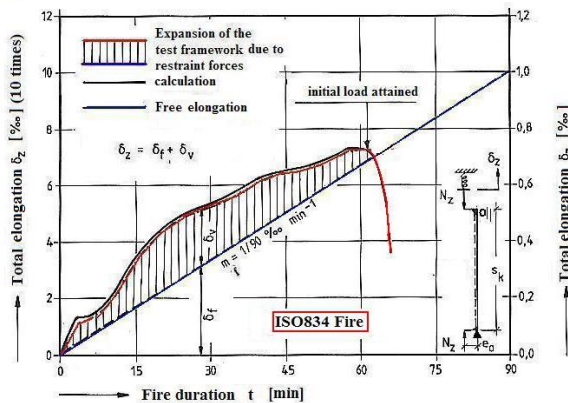


Figure 4.8: Total elongation of the framework due to free elongation and the restraining

Figure 4.8 shows the elongation of the test furnace due to the compression of the distance elements together allowed free elongation. The axial elongation of the test facility is again taken into account as additional free restraining in the calculation. As always, the lateral deformations of the (RFC) are determined by continuous measurements during the test. Figure 4.9

shows that the initial service load of the (RFC) is attained just before the 60th min. of fire development. After then initial load is kept constant until the fire resistance time is attained. Concerning restraint forces show a continuous decreasing after 25th min. of fire duration (red line curve in the Figure 4.8) as illustrated in the picture.

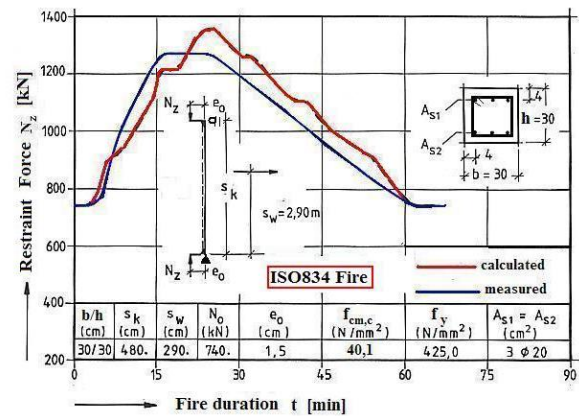


Figure 4.9: Measured and calculated restraint forces

Figure 4.9 shows a comparison of the measured and calculated restraint forces of the (RFC) in the fire test. The static and mechanical boundary conditions of the test specimen are given in a separate table in Figure 4.9. It can be seen that the calculated restraint forces are in good agreement with the test results during the entire fire duration.

The deformation behavior of the (RFC) is shown in Figure 4.10 together with the computation results. The comparison shows that, in this case also, the lateral deformations of the test specimen are well predicted. The computationally determined fire resistance is also confirmed by the failure time observed in the test. Calculation indicated a stability failure though in the test a material failure is observed.

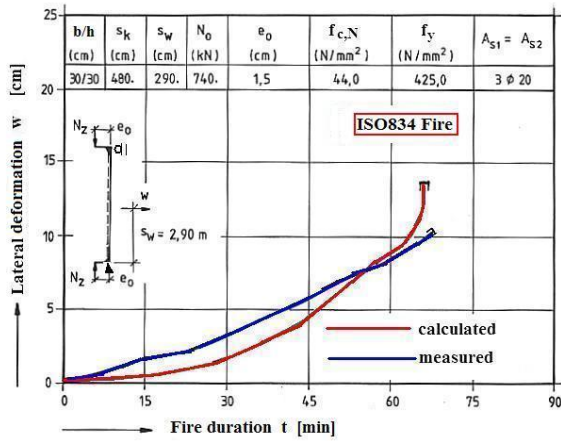


Figure 4.10: Measured and calculated lateral deformations

4.4. Column RS 84-1

In this test the hot-gas temperatures in the furnace differed from ISO834 and they are controlled according to a certain predetermined constant heating rate \dot{T}_f . Figure 4.11 shows the controlled temperature development. In the test heating rate \dot{T}_f is kept constant as 10 C/min. after an initial temperature disturbance zone in the furnace. This heating rate \dot{T}_f is chosen in order to show that the material model and the computation process can be applied also successfully for the other fire cases.

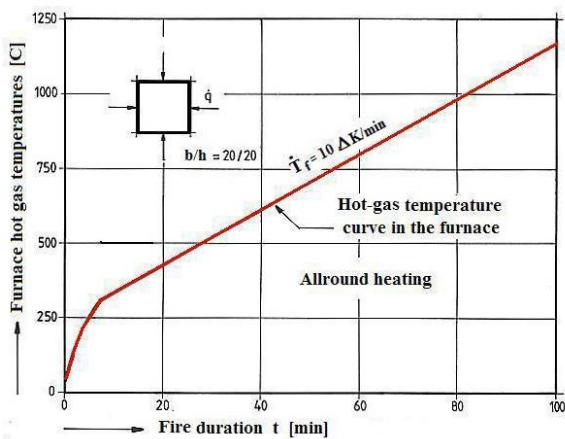


Figure 4.11: Predetermined furnace hot-gas temperatures as constant heating rate

Figure 4.12 shows the calculated and measured steel temperatures of the corner reinforcements in the (RFC) during the fire test. Since these steel reinforcements

are arranged symmetrically in the cross section, a single temperature development is determined by the calculation. A comparison of the predicted temperature development with the measured temperatures of the reinforcements clearly demonstrates that the temperature problem in the computer program has been simulated reliably.

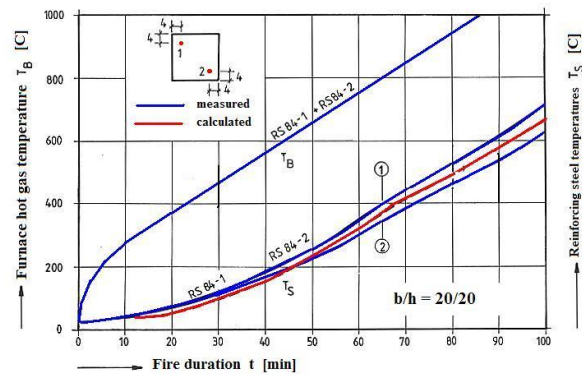


Figure 4.12: Developing of hot-gas temperatures and calculated and measured steel temperatures

In this test also a free restraint is applied as shown in Figure 4.13. It shows the predetermined free restraint of the (RFC) with respect to the fire duration (blue line). In the dashed area the further deformations of the test facility are shown bound to the measured restraint forces during the test. According to the illustration of the deformations of the framework, it becomes evident that the maximum restraint force is attained shortly before the 60th fire minute.

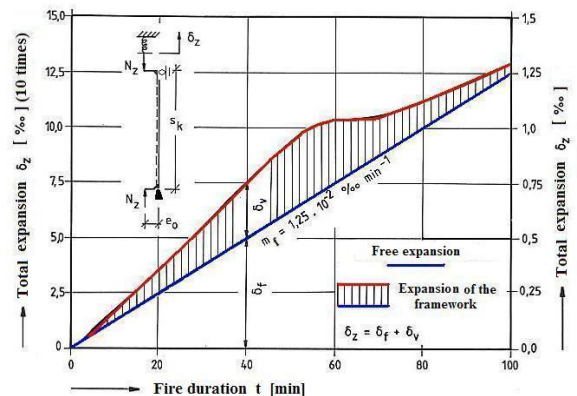


Figure 4.13: Total elongation of the framework due to free elongation and the restraining

Figure 4.14 illustrates the developing of the measured and predicted restraint forces of the (RFC) during the

fire. Obviously, the calculated restraint forces almost exactly reflect the test results. The calculation predicted no failure of the (RFC) even after almost two-hour fire duration. This prediction is also confirmed by the test.

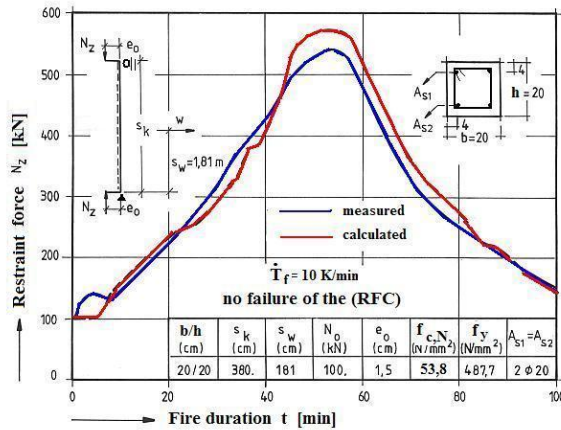


Figure 4.14: Measured and calculated restraint forces

For the restraint development of the test the analysis of [Eq. 38, 39] in *PART I* can give a clearing answer. At the beginning the creep deformations of (RFC) are low. The concrete has a comparatively high modulus of elasticity. In the [Eq. 38], the $R(t)$ has correspondingly low value, because this term is determined by the developing creep deformations during the fire. On the other hand, the term $Q(t)$ in [Eq. 39] controlled by the modulus of elasticity of the concrete, is relatively high. This combination results in an increase in the development of the restraint forces at the beginning of fire test. However, as the fire continues, considerable creep deformations appear with simultaneous reduction of the concrete E-modulus. These effects cause a regressive development of the functions $Q(t)$ and $R(t)$ which lead also to a decreasing stress development in the cross sections of (RFC). In addition, the increasing lateral deformations of the (RFC) make an additional contribution to the reduction of relaxation forces.

Figure 4.15 shows measured and calculated lateral deformations of (RFC) during the fire exposure. Although restraint forces are well reproduced, devia-

tions are observed in the lateral deformations which indicate the high creep effects in the calculation.

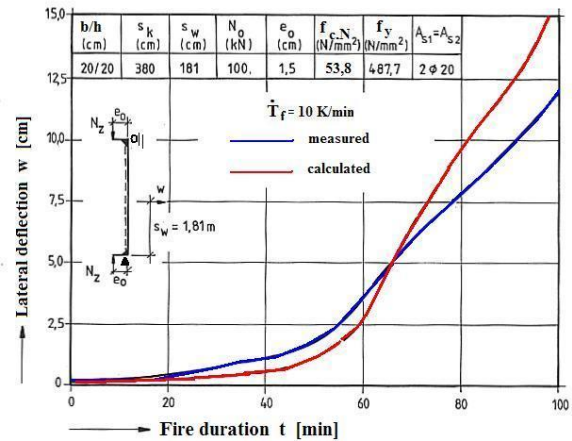


Figure 4.15: Measured and calculated lateral deformations

4.5. Column RS 84-3

In this fire test a (RFC) with a rectangular cross section ($b/h=30/40$) is used as specimen. The support line at the head and at the foot of the (RFC) is arranged eccentrically parallel to the shorter edge of the cross section. The buckling direction is thereby enforced in the direction of the weak cross section axis. In this test also a planned free restraint is applied as restraining condition.

Figure 4.16 shows the development of the axial free elongation of the (RFC) together with the furnace deformations. The blue line in the figure shows the simulated free restraint of the (RFC) during the ISO834 Fire test so; the red curve indicates the additional vertical deformation of the test facility. The planned free elongation is controlled in such a way that after reaching the 1‰ limit in the 90th minute of the fire exposure, this limit is maintained constant until the end of the test (blue line in Figure 4.16). The test is terminated after two-hour fire duration. No failure of the (RFC) is observed.

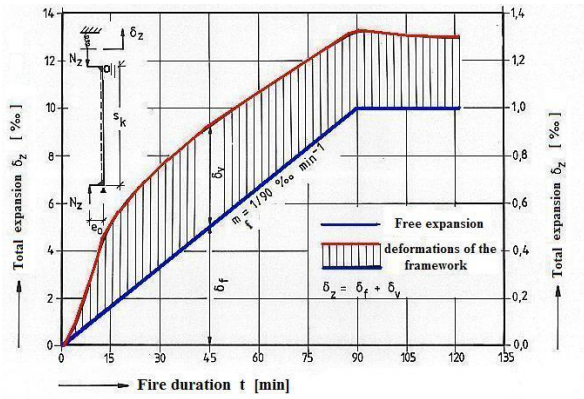


Figure 4.16: Total elongation of the framework due to free elongation and the restraining

In Figure 4.17, the measured and the calculated restraint forces of the test specimen are shown during the fire test. The mechanical and static boundary conditions of this (RFC) have been added to the figure in a table. The figure shows clearly that the time dependent development of the restraint forces is in good agreement with the calculation results together with the fire resistance.

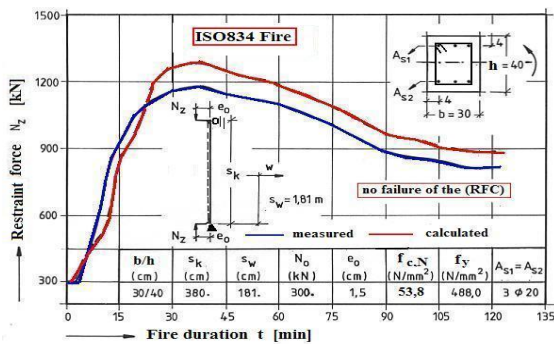


Figure 4.17: Measured and calculated restraint forces

The comparatively rapid increase of the restraint forces in this test is due to the static boundary conditions of the (RFC). The low slenderness and the small load eccentricity lead to this development, because the influences remain correspondingly small from the II. Order Theory. Nearly after 45th min. of fire duration the restraint forces show a falling development by the time which is incident of the creep effects due to the hot gas temperatures and stress condition in (RFC).

Figure 4.18 shows the development of lateral defor-

mations of (RFC) during the fire exposure. It can be seen from the illustration that the measured deformations increase up to the 30th min. of the fire duration. After then, however, no deformation changes could be recorded by the sensor. On the other hand, the calculation shows an increasing lateral deformation for the (RFC). Therefore, the possible test deformations of the (RFC) above this fire duration is estimated and drawn with dashed line in the Figure 4.18.

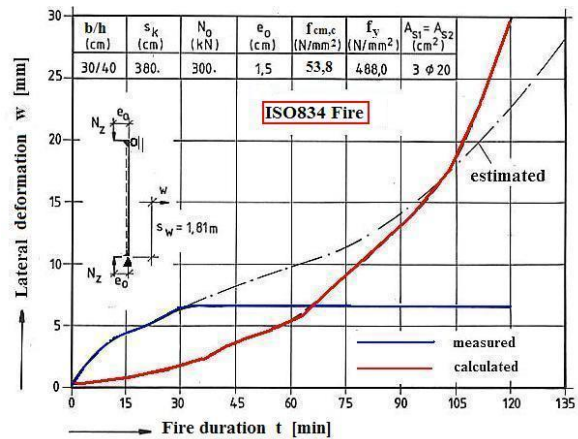


Figure 4.18: Measured and calculated lateral deformations

The test is ended arbitrarily after two hour fire duration because the continuation of the fire test would not bring additional information. The test aimed at the first hand obtaining the development of the lateral deformations and restraining forces during the fire (like RS84-1).

5. Conclusions

In SFB an intensive work is carried out to solve the *relaxation and creep* problems. In addition to the experimental research, a theoretical work is also carried out simultaneously on the development of a realistic material model (see PART I). It is emphasized that the material model for concrete and steel at high temperatures to be developed should, as far as possible, contain all influencing parameters for a realistic description of the fire behavior of reinforced concrete structures.

Various material models have been presented both in Germany and abroad. The use of these material models, in particular for describing the relaxation behavior of restrained (RFC), has up to now not led to a successful solution for the analysis of the test results. The new material model is developed by collaboration between the two subprojects (A and B3 of SFB) and its validity is confirmed by large scale tests as shown in the previous examples. This process is particularly important because the material models presented from researchers are valid only for certain and narrow boundary conditions and, above all, for assessment of the relaxation behavior of small specimens under fire condition.

The assessment of the fire behavior of structural elements made of reinforced concrete could only be achieved if the time-dependent material properties are taken into account as realistically as possible (see Anderberg, Y., 1983) In this process the influence of the heating rate \dot{T} of the concrete played a special role in the rheological model (Haksever, A., 1978-1980) At the same time, the load and time-dependent deformations of the concrete in the large scale structural elements are reformulated with the help of extensive experimental work. In this concern creep function in *PART I* has been described in stress, temperature and humidity dependent (see also Bazant, Z. P., Chern, J. C., 1988).

The calculation program used naturally requires a great deal of numerical treatment. Since the determination of the stresses and deformations components must be successively calculated, it is inevitable that the time steps are to select very small for carrying out a load bearing analysis for the entire fire duration. In the cases in which relatively fast deformation and stress changes can be expected, the reduction of time steps are particularly indicated. The calculations have shown that a time step limit of 3-5 minutes should not be exceeded in case of restraining (RFC).

Despite the good agreement between the test and the calculation results, it cannot be said that for the restraint problem of reinforced concrete elements in case of fire the research activities should be ended. Special attention must be given in the future to the transfer of the material laws from small test specimens on large scale test elements (Haksever, A, 1984-1986, Gesamtverformung).

Acknowledgement: The Deutsche Forschungsgemeinschaft (German Research Foundation; DFG) who supported the research works of SFB, where the author was also active for many years, deserves particular thanks and appreciates.

Notations

| | | |
|----------------------------|---|--|
| A_{sI} | Tensile reinforcing | [mm ²] |
| A_{s2} | Compressive reinforcing | [mm ²] |
| a | Thermal diffusivity of normal concrete (see appendix) | [m ² /h] |
| b | Width of the cross section of (RFC) | [mm] |
| C_K | Convection constant (see appendix) | [W.s ^{1/2} /m ^{3/2} K] |
| c | Heat capacity (see appendix) | [kW.s/kgK] |
| h | Depth of the cross section of (RFC) | [mm] |
| E_{20} | Modulus of elasticity of concrete at room temperatures (see appendix) | [N/mm ²] |
| E_T | Modulus of elasticity of concrete at elevated temperatures (see appendix) | [N/mm ²] |
| e_0 | Eccentricity of the vertical load | [cm] |
| f | Strength | [N/mm ²] |
| f_y | Yield strength of steel | [N/mm ²] |
| $f_{cm,cube} = f_{cm,c}$ | Mean concrete cube compressive strength of 28 days at room temperatures | [N/mm ²] |
| $f_{cm,cubeT} = f_{cm,cT}$ | Mean concrete cube compressive strength at elevated temperatures | [N/mm ²] |
| f_{ck} | Characteristic concrete strength | [N/mm ²] |
| l | Length | [mm] |
| m_f | Free elongation rate of the restraining | [%/min] |
| N | Vertical load of (RFC) | [kN] |
| N_0 | Initial vertical load of (RFC) | [kN] |

| | | | |
|-------------|---|---------------------|--|
| N_z | Restraint force | [kN] | Pages 1-11. |
| | Heat flow direction | ← | Bazant, Z.P.; Chern, J.C.: Concrete Creep at Variable Humidity: Constructive Law and Mechanism. <i>Mat. et Constr.</i> , Vol.18, No.103, 1/20, 1985. |
| \dot{q}_T | Total Heat flow (see appendix) | [W/m ²] | |
| \dot{q}_K | Convective heat flow (see appendix) | [W/m ²] | David Lange, Johan Sjöström.: Mechanical response of a partially restrained column exposed to localized fires. <i>Fire Safety Journal</i> , Volume 67, July 2014, Pages 82-95. |
| \dot{q}_R | Heat flow by radiation (see appendix) | [W/m ²] | |
| s_k | Buckling length of the (RFC) | [cm, m] | DIN 4102 – Brandverhalten von Baustoffen und Bauteilen (Fire behavior of building materials and structural elements) Teile (Parts) 1-3, Teile 5-7, and Teil 4., DIN Deutsches Institut für Normung E.V., Beuth Verlag, Berlin, (1981) |
| s_w | The height for the measured and calculated lateral deformation of (RFC) | [m] | |
| T_g | Hot-gas temperature in the furnace | [C] | DIN V ENV 1992-1-2 Eurocode 2 – Planung von Stahlbeton- und Spannbeton-tragwerken, Teil 1-2: Allgemeine Regeln – Tragwerksbemessung für den Brandfall, (Design of structural constructions for fire exposure), (1997). |
| T_s | Reinforcing steel temperatures | [C] | |
| \dot{T}_f | Heating rate of the furnace | [C/min] | |
| T | Temperature | [C] | Haksever, A.: Zum Relaxationsverhalten von Stahlbetonstützen im Brandfall. SFB Jahresbericht 1981-1983, Teil I (On the relaxation behavior of reinforced concrete columns in case of fire, SFB, Report) Technische Universität Braunschweig. |
| ΔK | Kelvin difference | [C] | |
| T_L | Local Temperature | [C] | |
| T_w | Surface temperature (see appendix) | [C] | |
| t | Time | [min, s] | Haksever, A.: Relaxationsverhalten von Stahlbeton-tragwerke im Brandfall. SFB Jahresbericht 1978-1980, Teil I (Relaxation behaviour of reinforced concrete structures), Technische Universität Braunschweig. |
| v_g | Hot gas flow velocity on the surface of (RFC) | [m/s] | |
| w | Lateral deformation | [cm] | Haksever, A.: Mathematische Modellierung des Verformungsverhaltens von Festbetone unter Brandbeanspruchung. SFB Jahresbericht 1984-1986, Teil I (Mathematical description of deformation behavior hard concrete), Technische Universität Braunschweig. |
| w_h | Humidity (see appendix) | [%] | |
| w/c | Water/cement ratio (see appendix) | [-] | |

Additional Symbols

| | | | |
|------------------|---|-------------------------------------|--|
| α_i | Heat transfer coefficient in the furnace (see appendix) | [W/m ² K] | Haksever, A.: Gesamtverformung der Großbeton-Probekörper im Brandfall. SFB Jahresbericht 1984-1986, Teil I (Total deformation large scale specimens in case of fire., SFB, Report 1984-1986, Part I), Technische Universität Braunschweig. |
| δ_z | Total elongation | [%] | ISO: International Organization for Standardization ISO Central Secretariat. Chemin de Blandonnet 8, CP 401. 1214 Vernier, Geneva, Switzerland |
| δ_f | Free elongation for the (RFC) | [%] | |
| δ_v | Elongation of the test framework due to retraining forces | [%] | I. Cabrita Neves, J.C. Valente, J.P. Correia Rodrigues.: Thermal restraint and fire resistance of columns. <i>Fire Safety Journal</i> , Volume 37, Issue 8, November 2002, Pages 753-771. |
| ϵ_{res} | Resulting emission factor (see appendix) | | |
| λ | Heat conductivity (see appendix) | [W/mK] | Kang-Hai Tan, Truong-Thang Nguyen.: Structural responses of (RFC) subjected to uniaxial bending and restraint at elevated temperatures. <i>Fire Safety Journal</i> , Volume 60, (2013), 1-13. |
| σ | Stefan-Boltzmann constant (see appendix) | [W/m ² .K ⁴] | |
| ρ | Density | [kg/m ³] | Kang-Hai Tan, Truong-Thang Nguyen.: Thermal-induced restraint forces in reinforced concrete columns subjected to eccentric loads. <i>Fire Safety Journal</i> , Volume 69, (2014), 136-146 |

References

Anderberg, Y.: Fire-Exposed Hyperstatic Concrete Structures- A Testal and Theoretical Study. Div. of Structural- Mechn. And Concrete Constr., Inst. of Techn., Lund, 1976.

Anderberg, Y.: Stress and Deformation characteristics of Concrete in high Temperatures. RILEM-Committee 44-PHT, Febr. 1983.

António José P. Moura Correia, João Paulo C. Rodrigues.: Fire resistance of steel columns with restrained thermal elongation. *Fire Safety Journal*, Volume 50, May 2012,

Klingsch, W., Traglastberechnung instationär thermisch belasteter Stahlbeton-Druck-glieder (Load bearing calculation of reinforced concrete compression elements under instationary thermic loading). Diss., Technische Universität Braunschweig, 1975.

Kordina, K., Meyer-Ottens, C.: Beton-Brandschutz Handbuch, (Concrete-Fire Protection Handbook), Beton-Verlag GmbH, Düsseldorf 1981. ISBN-3-7640-0136-4.

P. Bamonte, F. Lo Monte.: Reinforced concrete columns exposed to standard fire: Comparison among different constitutive models for concrete at high temperature. Fire Safety Journal, Volume 71, January 2015, Pages 310-323.

Schneider, U.: Behavior of Concrete at High Temperatures. Deutscher Ausschuss für Stahlbeton, Heft 337, Verlag W. Ernst und Sohn, Berlin, 1982.

Schneider, U.: Creep and Relaxation of Concrete under High Temperatures (in German). Habilitation, Technische Universität Braunschweig, 1979.

Schneider, U., Haksever, A.: Wärmobilanzrechnungen für Brandräume (Heat balance calculations for fire rooms). Technische Universität Braunschweig, IBMB, 1980.

SFB 148.: "Sonderforschungsbereich 148, Brandverhalten von Bauteilen" (A special research field Nr. 148, Fire behavior of structural elements).

Subproject A: Fire behavior of structural elements

Subproject B3: Material behavior of structural concrete elements at elevated temperatures.

Technische Universität Braunschweig, Germany. 1971-1986.

APPENDIX

In appendix, illustrations are given for the calculation of the temperature distribution as well as thermal material properties of concrete for the calculation of fire behavior of the (RFC) which are used in the computational research.

A) Thermal properties of normal concrete for heat transfer calculation (Kordina, K. et al. 1988).

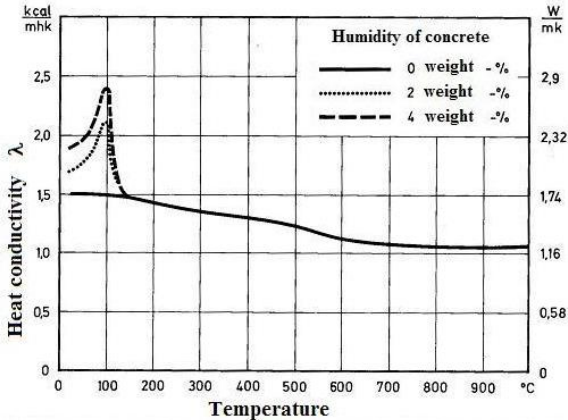


Figure A1: Heat conductivity of concrete λ with quartzite aggregate at elevated temperatures

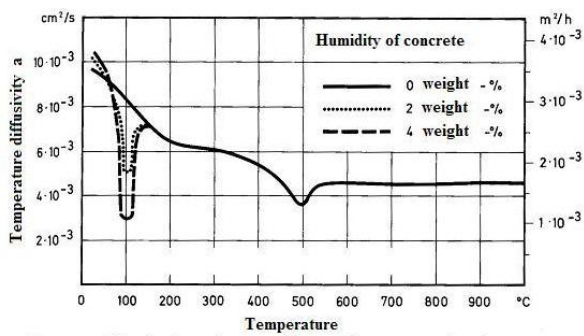


Figure A2: Thermal diffusivity of concrete a with quartzite aggregate at elevated temperatures

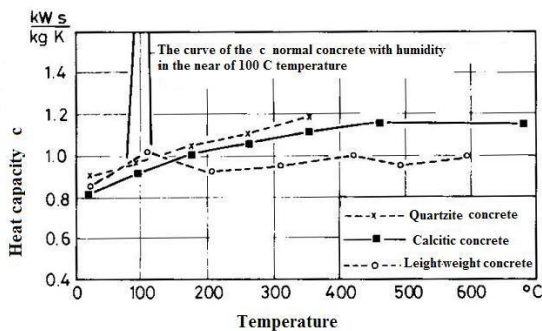


Figure A3: Specific heat capacity of concrete c with different aggregates at elevated Temperatures

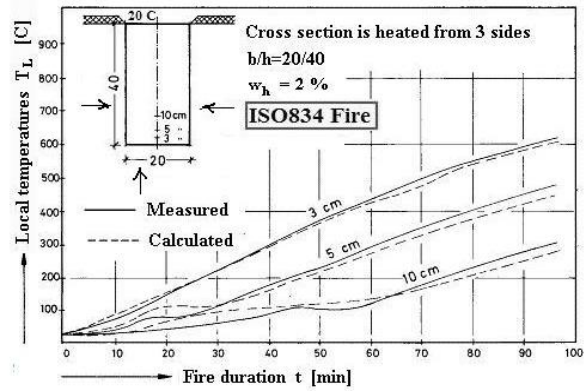


Figure A4: Comparison of measured and calculated temperatures of a concrete beam

B) Thermal material properties of concrete

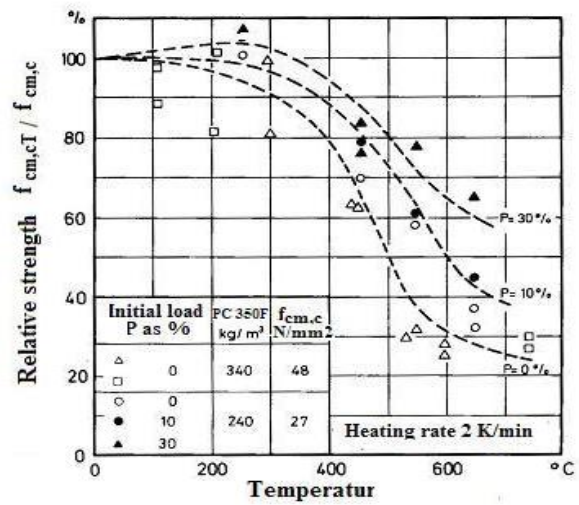


Figure B1: Relative strength of concrete with quartzite aggregate under different initial loads at elevated temperatures

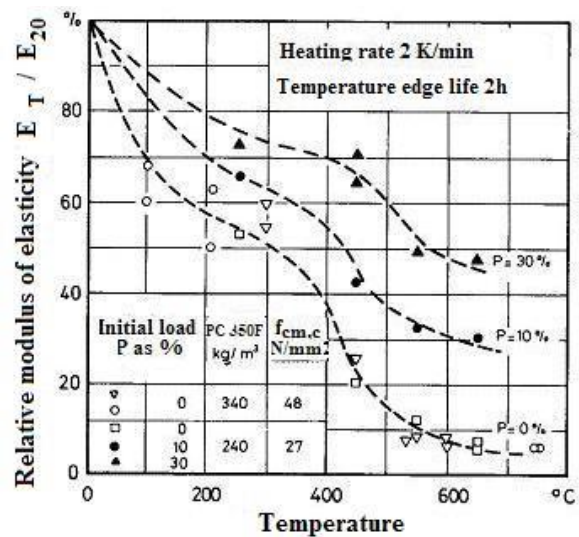


Figure B2: Relative modulus of elasticity of concrete with quartzite aggregate at elevated temperatures

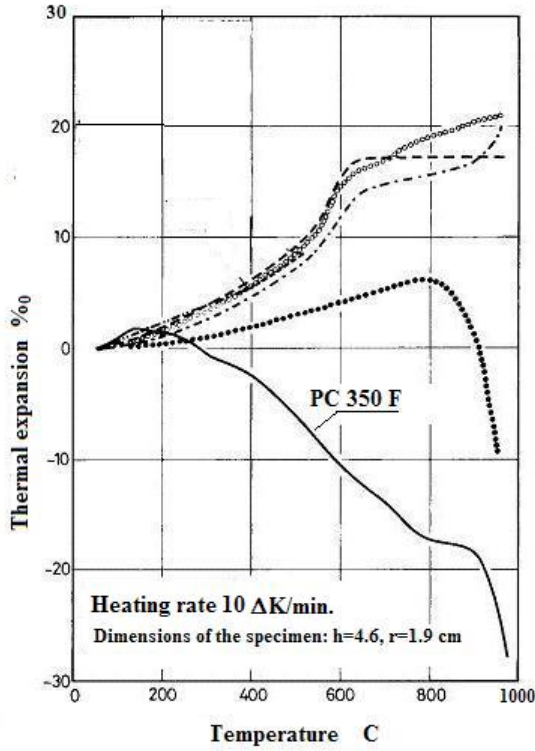


Figure B3: Thermal elongation of concrete with different aggregates at elevated temperatures

C) Heat transfer in the furnace. (Schneider, U., et al., 1980).

Total heat transfer density to the (RFC) through convection and radiation \dot{q}_T :

The following equations are applied for both the ISO834 Fire as well as the constant heating rate (as in this article). Fundamental equations are given below:

C1) Total heat energy density

$$\dot{q}_T = \alpha_i (T_g - T_w) + \epsilon_{res} \sigma (T_g^4 - T_w^4) = \dot{q}_K + \dot{q}_R \quad [\text{W/m}^2] \quad (1)$$

C1.1) Convective heat energy density

$$\alpha_i = \frac{7}{6} (7.38 + 0.00224 T_g) v_g^{0.5} = C_K v_g^{0.5} \quad [\text{W/m}^2\text{K}] \quad (2)$$

$$\dot{q}_K = \alpha_i (T_g - T_w) \quad [\text{W/m}^2]$$

$v_g \approx 5 \text{ m/s}$ is set in the calculations

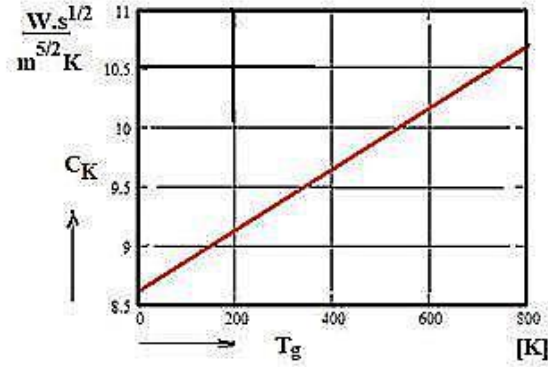


Figure C1: Coefficient C_K in Eq. 2 bound to the temperature

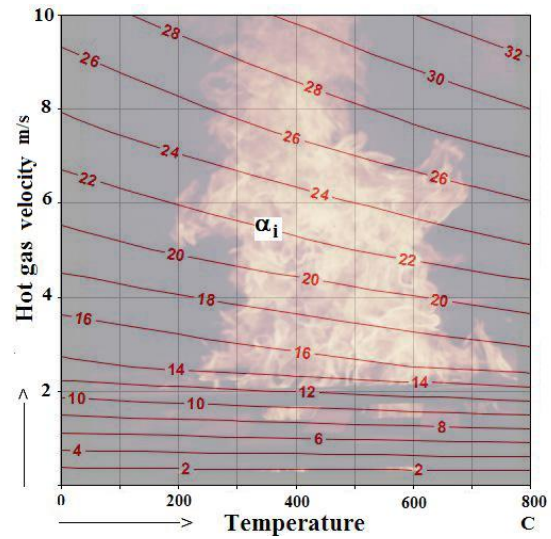


Figure C2: Convection factor α_i in Eq. 2 $\text{W/m}^2\text{K}$ bound to the temperature and hot gas velocity

C1.2) Radiant heat energy density

$$\dot{q}_R = \epsilon_{res} \sigma (T_g^4 - T_w^4) \quad (3)$$

$$\epsilon_{res} = \epsilon_g \cdot \epsilon_w = 0.35 \quad (4)$$

ϵ_g Hot gas emission, ϵ_w emission of the concrete surface

$$\sigma = 5.67 \cdot 10^{-8} \text{ W/m}^2 \cdot \text{K}^4 \quad (5)$$

Temperature distribution in the (RFC)-section is calculated using the Fourier-Equation:

$$\frac{\partial T}{\partial t} = \frac{\lambda}{\rho c} \left(\frac{\partial^2 T}{\partial x^2} + \frac{\partial^2 T}{\partial y^2} \right) + \frac{d\lambda}{dT} \left[\left(\frac{\partial T}{\partial x} \right)^2 + \left(\frac{\partial T}{\partial y} \right)^2 \right] \quad (6)$$

In equation (6) any heat sources in (RFC) are excluded. For a plane surface x, y shows the coordinates of the calculated temperatures at discrete points. Thermal material properties a, c and λ are taken into account as a function of temperature by means of linear approximations (see Figures A1-A3).